Published in final edited form as:
Oncogene. 2011 April 21; 30(16): 1956–1962. doi:10.1038/onc.2010.568.

Long non-coding RNA *ANRIL* is required for the PRC2 recruitment to and silencing of *p15*^{INK4B} tumor suppressor gene

Y Kotake[1,2], **T Nakagawa**[2], **K Kitagawa**[1], **S Suzuki**[1], **N Liu**[1], **M Kitagawa**[1], and **Y Xiong**[2,3]

[1]Department of Biochemistry 1, Hamamatsu University School of Medicine, Shizuoka, Japan

[2]Lineberger Comprehensive Cancer Center, Department of Biochemistry and Biophysics, Program in Molecular Biology and Biotechnology, University of North Carolina at Chapel Hill, Chapel Hill, NC, USA

[3]Department of Biochemistry and Biophysics, Program in Molecular Biology and Biotechnology, University of North Carolina at Chapel Hill, Chapel Hill, NC, USA

Abstract

A 42 kb region on human chromosome 9p21 encodes for three distinct tumor suppressors, p16^{INK4A}, p14^{ARF} and p15^{INK4B}, and is altered in an estimated 30–40% of human tumors. The expression of the *INK4A-ARF-INK4B* gene cluster is silenced by polycomb during normal cell growth and is activated by oncogenic insults and during aging. How the polycomb is recruited to repress this gene cluster is unclear. Here, we show that expression of oncogenic Ras, which stimulates the expression of *p15*^{INK4B} and *p16*^{INK4A}, but not *p14*^{ARF}, inhibits the expression of *ANRIL* (antisense non-coding RNA in the *INK4* locus), a 3.8 kb-long non-coding RNA expressed in the opposite direction from *INK4A-ARF-INK4B*. We show that the *p15*^{INK4B} locus is bound by SUZ12, a component of polycomb repression complex 2 (PRC2), and is H3K27-trimethylated. Notably, depletion of *ANRIL* disrupts the SUZ12 binding to the *p15*^{INK4B} locus, increases the expression of *p15*^{INK4B}, but not *p16*^{INK4A} or *p14*^{ARF}, and inhibits cellular proliferation. Finally, RNA immunoprecipitation demonstrates that *ANRIL* binds to SUZ12 *in vivo*. Collectively, these results suggest a model in which *ANRIL* binds to and recruits PRC2 to repress the expression of *p15*^{INK4B} locus.

Keywords

long non-coding RNA; *ANRIL*; polycomb; p15^{INK4B}; p16^{INK4A}; ARF

Introduction

The *INK4A-ARF-INK4B* gene cluster occupies a 42 kb stretch on the human chromosome 9p21 and is homozygously deleted or expression silenced in a wide range of human cancers with an estimated frequency of ~40% (Sherr, 1998; Kim and Sharpless, 2006), representing one of the most frequently altered genes in human cancer. Genetic analyses in mice with

Correspondence: Dr M Kitagawa, Department of Biochemistry 1, Hamamatsu University School of Medicine, 1-20-1 Handayama, Higashi-ku, Hamamatsu, Shizuoka 431-3192, Japan. kitamasa@hama-med.ac.jp or Dr Y Xiong, Lineberger Comprehensive Cancer Center, Department of Biochemistry and Biophysics, Program in Molecular Biology and Biotechnology, University of North Carolina at Chapel Hill, Chapel Hill, NC 27599, USA. yxiong@email.unc.edu.

Conflict of interest

The authors declare no conflict of interest.

Supplementary Information accompanies the paper on the Oncogene website (http://www.nature.com/onc)

mutations targeting each gene individually support the tumor suppression function for all three genes (Serrano *et al.*, 1996; Kamijo *et al.*, 1997; Krimpenfort *et al.*, 2001, 2007; Sharpless *et al.*, 2001). Of these three tumor suppressors encoded by this gene cluster, both $p15^{INK4B}$ and $p16^{INK4A}$ function as the inhibitors of CDK4 and CDK6, and thereby retain the growth suppressive activity of RB family proteins, whereas ARF, expressed from a distinct promoter and an alternative reading frame of *INK4A*, binds to and inhibits the activity of oncoprotein MDM2 and thus stabilizes and activates p53. Clustering three distinct growth and tumor suppressors in such a small region may aid the coordinated integration of different growth insults into two major tumor suppression pathways in mammalian cells, one mediated by RB and the other by p53 (Gil and Peters, 2006).

All the three genes are expressed at a barely detectable low level in young and normal cells, and are accumulated during cell aging or in cells insulted by hyperproliferative oncogenic stimuli (Zindy *et al.*, 1997; Krishnamurthy *et al.*, 2004; Gil and Peters, 2006), suggesting a common cellular mechanism and potentially coordinated regulation of these three genes—to maintain aged cells in senescence and to arrest oncogenic-insulted cells from proliferation.

The repression of this gene cluster involves polycomb proteins and histone H3 lysine27 (H3K27) trimethylation (Jacobs *et al.*, 1999; Itahana *et al.*, 2003; Bracken *et al.*, 2007; Kotake *et al.*, 2007; Kia *et al.*, 2008; Agger *et al.*, 2009). The polycomb proteins form multimeric protein complexes, PRC (polycomb repression complex)-1 and -2 that are involved in the heritable stable repression of genes through histone modification. Previous genetic and biochemical studies suggest a hierarchical recruitment model where PRC2-mediated H3K27 methylation is required for recruitment of PRC1, which causes H2A-K119 ubiquitination on the *Hox* gene cluster both in fly and human cells (Wang *et al.*, 2004; Cao *et al.*, 2005). A critical issue for better understanding the regulation of the *INK4A-ARF-INK4B* gene cluster is how PRC1 and PRC2 are recruited to this region.

Several long non-coding RNAs (lncRNAs) have recently been reported to have a direct role in recruiting PRC2 complexes to specific loci and repress gene expression. These include *RepA*, a 1.6-kb lncRNA involved in X-chromosome inactivation (Zhao *et al.*, 2008), *Kcnq1ot1*, a 91.5 kb lncRNA required for 10 paternally imprinted genes on 11p15 (Pandey *et al.*, 2008; Terranova *et al.*, 2008; Zhao *et al.*, 2008), and *HOTAIR*, a 2.2-kb ncRNA involved in the repression of the *HOX* loci and promoting cancer metastasis (Rinn *et al.*, 2007; Gupta *et al.*, 2010). These findings led us to explore the possibility that *ANRIL* (antisense non-coding RNA in the *INK4* locus), a 3834 bp transcript whose transcription is initiated from the *INK4A-ARF-INK4B* gene cluster (Figure 1a), may be involved in the repression of *INK4A*, *ARF* and/or *INK4B*. *ANRIL* contains 19 exons, a polyadenylation site in the last exon and spans over 126 kb of genomic sequence that is deleted in the melanoma–neural system tumor syndrome family analyzed by previous study (Pasmant *et al.*, 2007). Exon 1 of *ANRIL* locates between the promoter of *ARF* and *INK4B*, and is transcribed in the direction opposite from that of $p15^{INK4B}$. Deletion of a 70-kb sequence in mouse chromosome 4 synteny to a 58-kb non-coding region in human chromosome 9p21 that includes seven exons of *ANRIL* resulted in a significantly increased expression of both $p16^{INK4A}$ and $p15^{INK4B}$ in several organs and tissues, but had no effect on other neighboring genes (Visel *et al.*, 2010), providing a genetic evidence for the negative regulation of $p16^{INK4A}$ and $p15^{INK4B}$ by the ncRNA sequences expressed in this region. In this report, we show that $p15^{INK4B}$ locus is repressed by PRC2 proteins and that *ANRIL* is required for the recruitment of PRC2 to and repression of the $p15^{INK4B}$ locus.

Results and discussion

We first determined the expression of *ANRIL* in response to two well-characterized oncoproteins, E7 and Ras, which are known to affect the expression of $p16^{INK4A}$, *ARF* and/or $p15^{INK4B}$. Although E7 inactivates RB family proteins and potently activates the expression of $p16^{INK4A}$ and to a lesser extent $p14^{ARF}$ (Kotake *et al.*, 2007, 2009), oncogenic Ras induces the expression of $p15^{INK4B}$ (Malumbres *et al.*, 2000) (Figures 1b and c). We established stable cell lines expressing either E7 or oncogenic Ras^{G12V} and determined the expression of these tumor suppressor genes as well as *ANRIL*. As expected, both $p16^{INK4A}$ and $p14^{ARF}$ mRNAs, but not $p15^{INK4B}$, were substantially increased in WI38/E7 cells, whereas in WI38/Ras^{G12V} cells, $p15^{INK4B}$ and $p16^{INK4A}$, but not $p14^{ARF}$, was stimulated by more than 12-fold ($p15^{INK4B}$) and 2-fold ($p16^{INK4A}$) (Figures 1b and c). The induction of $p16^{INK4A}$ by Ras^{G12V} in WI38 cells is somewhat lower than that seen in some other normal fibroblast such as MEFs or IMR-90. The reason for this is not clear, but may relate to the difference between species or cell lines. The expression of *ANRIL* was readily detectable in WI38 cells, was not significantly affected by the expression of E7 and was notably reduced by the expression of H-Ras^{G12V} (Figure 1c). These data indicate that stimulation of $p15^{INK4B}$ by oncogenic Ras in cultured normal human cells is associated with a decrease of *ANRIL* expression, suggesting a potential negative regulation of $p15^{INK4B}$ by *ANRIL*.

We then designed a retroviral vector encoding a short hairpin RNA that specifically targets the exon1 region of *ANRIL*. Infection of WI38 cells with *ANRIL* short hairpin RNA retroviruses efficiently reduced *ANRIL* level (Figure 2a). Quantitative reverse transcriptase PCR analysis showed that silencing *ANRIL* resulted in an increase of $p15^{INK4B}$ expression by nearly 8-fold, but had minimal effect on the expression of $p16^{INK4A}$ (increased by 1.8-fold) or $p14^{ARF}$ (reduced by half, Figure 2b). Similar result was also reported very recently by Yap *et al.* that silencing *ANRIL* by a different method using antisense DNA increases the $p16^{INK4A}$ expression four-fold in another normal human diploid fibroblasts line, IMR-90 cells (Yap *et al.*, 2010). Associated with $p15^{INK4B}$ increase, *ANRIL* silencing also resulted in decreased cell growth (Figure 2c) and an increase of cells stained positively for senescence-associated β-galactosidase activity, an indicator of cell senescence (Figure 2d). These results indicate that *ANRIL* is involved in the selective repression of $p15^{INK4B}$ transcription and prevention of cellular senescence. To search for the mechanism underlying the repression of $p15^{INK4B}$ by *ANRIL*, we examined the role of PRC2 in $p15^{INK4B}$ regulation. Transduction of WI38 cells with a retroviral vector encoding an short hairpin RNA targeting the catalytic subunit of PRC2 histone methyltransferase, *EZH2*, efficiently reduced *EZH2* level (Figure 3a). Associated with *EZH2* decrease is a substantial increase of $p15^{INK4B}$ mRNA by eightfold and $p16^{INK4A}$ mRNA by threfold, but no detectable effect on $p14^{ARF}$ mRNA level (Figure 3b). Associated with increase of $p15^{INK4B}$ and $p16^{INK4A}$, *EZH2* knockdown decreased cell growth (Figure 3c) and induced cell senescence (Figure 3d). To further confirm this, we transfected WI38 cells with small interfering RNA silencing *SUZ12*, another component of PRC2, and found that silencing SUZ12 (Figure 3e) also increased the expression of both $p15^{INK4B}$ as well as $p16^{INK4A}$ expression (Figure 3f). These results indicate that PRC2 is involved in the $p15^{INK4B}$ repression and cellular senescence.

That both *ANRIL* and PRC2 repress $p15^{INK4B}$ expression led us to determine whether *ANRIL* is required for PRC2 recruitment to $p15^{INK4B}$ locus. We first carried out a chromatin immunoprecipitation assay to test whether PRC2 directly binds to the $p15^{INK4B}$ locus. This assay demonstrated that the $p15^{INK4B}$, as well as $p16^{INK4A}$, locus is bound by SUZ12 and is trimethylated at lys27 of histone H3 (Figure 4a). Chromatin immunoprecipitation–quantitative PCR assay showed that silencing *ANRIL* causes substantial loss of SUZ12 occupancy on the $p15^{INK4B}$ locus (Figure 4c), although the steady state level of the SUZ12 protein is unchanged (Figure 4b). Finally, we examined whether *ANRIL* binds directly to

SUZ12 by RNA immunoprecipitation assay and found that the SUZ12 immunocomplex, but not the immunocomplexes of immunoglobulin G or another negative control YY1, substantially enriched *ANRIL* RNA compared with *U1* RNA, a non-specific RNA that is expressed in the cells at high levels (Figure 4d). These results demonstrate that *ANRIL* can bind directly and specifically to SUZ12.

In this report, we showed that mRNA-like ncRNA, *ANRIL*, and the PRC2 histone methyltransferase complex are involved in the repression of $p15^{INK4B}$ transcription. We further demonstrated that *ANRIL* binds to SUZ12, a PRC2 component, and is required for the SUZ12 occupancy on the $p15^{INK4B}$ locus. Loss of *ANRIL* or PRC2 showed the same effects on cellular proliferation and both cause premature senescence, supporting a mechanistic link between PRC2 and *ANRIL*. The results presented herein provide new insight into the epigenetic control of $p15^{INK4B}$ locus by PRC2 and lncRNA. The detailed biochemical mechanisms underlying the function of *ANRIL* in the PRC2 recruitment to the $p15^{INK4B}$ locus remain to be determined including, in particular, the interaction between *ANRIL* and PRC2. The other ncRNA, *Xist*, directly associates with EZH2 through RepA, a motif comprising 7.5 tandem repeats of a 28-nucleotide sequence that folds into two conserved stem-loop structures (Wutz *et al.*, 2002; Zhao *et al.*, 2008). Although we could not find such a distinctive motif on *ANRIL*, we showed the direct binding between *ANRIL* and PRC2. A recent study utilized high-magnification RNA–DNA FISH assay to demonstrate that large ncRNA, *Air*, interacts with the chromatin of cis-linked target gene promoter and recruits the H3K9 histone methyltransferase to repress the gene expression (Nagano *et al.*, 2008). Based on that, *ANRIL* may directly interact with the $p15^{INK4B}$ promoter chromatin to recruit PRC2. Very recently, Yap *et al.* reported that CBX7, an H3k27me3-recognizing component of PRC1, can bind directly to both *ANRIL* and H3K27me3 via its chromodomain, and both interactions are required for CBX7 to repress the *INK4A* and *INK4B* loci (Yap *et al.*, 2010). In the present study, we demonstrated that *ANRIL* is also involved in the recruitment of another polycomb complex, PRC2, to another gene, $p15^{INK4B}$, in the *INK4A-ARF-INK4B* region. Our study thus broadens the scope of *ANRIL* function. Given that *ANRIL* encodes an almost 4 kb ncRNA that binds at least two different polycomb proteins, it will be important to determine the responsible regions in *ANRIL* for the association with each polycomb protein.

Recent genome-wide association studies have linked common single-nucleotide polymorphisms in 9p21 region that is independently associated with both type II diabetes and coronary heart disease (Helgadottir *et al.*, 2007; McPherson *et al.*, 2007; Saxena *et al.*, 2007; Scott *et al.*, 2007). As the *ANRIL* genomic region spans the risk-associated single-nucleotide polymorphisms (Broadbent *et al.*, 2008), expression of *ANRIL* might be affected by the unknown causative genetic variant. Therefore, it is possible that the deregulation of *ANRIL* by such risk-associated single-nucleotide polymorphisms changes the expression level of $p15^{INK4B}$ and/or other target genes, leading to the development of type II diabetes or coronary heart disease in humans.

Supplementary Material

Refer to Web version on PubMed Central for supplementary material.

Acknowledgments

We thank Howard Chang for the insightful discussion during this study, Yaxue Zeng and Matt Smith for helpful discussion and reading the manuscript, Mika Matsumoto, Michiyo Hakamata and Harumi Shiratori for technical assistance. This study is supported by grants from the Ministry of Education, Science, Sports, Culture, and Technology of Japan (YK, MK, SS and KK) and NIH grant CA68377 (YX).

References

Agger K, Cloos PA, Rudkjaer L, Williams K, Andersen G, Christensen J, et al. The H3K27me3 demethylase JMJD3 contributes to the activation of the INK4A-ARF locus in response to oncogene- and stress-induced senescence. Genes Dev. 2009; 23:1171–1176. [PubMed: 19451217]

Bracken AP, Kleine-Kohlbrecher D, Dietrich N, Pasini D, Gargiulo G, Beekman C, et al. The polycomb group proteins bind throughout the INK4A-ARF locus and are disassociated in senescent cells. Genes & Dev. 2007; 21:525–530. [PubMed: 17344414]

Broadbent HM, Peden JF, Lorkowski S, Goel A, Ongen H, Green F, et al. Susceptibility to coronary artery disease and diabetes is encoded by distinct, tightly linked SNPs in the ANRIL locus on chromosome 9p. Hum Mol Genet. 2008; 17:806–814. [PubMed: 18048406]

Cao R, Tsukada Y, Zhang Y. Role of Bmi-1 and Ring1A in H2A ubiquitylation and *Hox* gene silencing. Mol Cell. 2005; 20:845–854. [PubMed: 16359901]

Gil J, Peters G. Regulation of the INK4b-ARF-INK4a tumour suppressor locus: all for one or one for all. Nat Rev Mol Cell Biol. 2006; 7:667–677. [PubMed: 16921403]

Gupta RA, Shah N, Wang KC, Kim J, Horlings HM, Wong DJ, et al. Long non-coding RNA HOTAIR reprograms chromatin state to promote cancer metastasis. Nature. 2010; 464:1071–1076. [PubMed: 20393566]

Helgadottir A, Thorleifsson G, Manolescu A, Gretarsdottir S, Blondal T, Jonasdottir A, et al. A common variant on chromosome 9p21 affects the risk of myocardial infarction. Science. 2007; 316:1491–1493. [PubMed: 17478679]

Itahana K, Zou Y, Itahana Y, Martinez JL, Beausejour C, Jacobs JJ, et al. Control of the replicative life span of human fibroblasts by p16 and the polycomb protein Bmi-1. Mol Cell Biol. 2003; 23:389–401. [PubMed: 12482990]

Jacobs JJ, Kieboom K, Marino S, DePinho RA, van Lohuizen M. The oncogene and polycomb-group gene bmi-1 regulates cell proliferation and senescence through the ink4a locus. Nature. 1999; 397:164–168. [PubMed: 9923679]

Kamijo T, Zindy F, Roussel MF, Quelle DE, Downing JR, Ashmun RA, et al. Tumor suppression at the mouse INK4a locus mediated by the alternative reading frame product $p19^{ARF}$. Cell. 1997; 91:649–659. [PubMed: 9393858]

Kia SK, Gorski MM, Giannakopoulos S, Verrijzer CP. SWI/SNF mediates polycomb eviction and epigenetic reprogramming of the INK4b-ARF-INK4a locus. Mol Cell Biol. 2008; 28:3457–3464. [PubMed: 18332116]

Kim WY, Sharpless NE. The Regulation of INK4/ARF in cancer and aging. Cell. 2006; 127:265–275. [PubMed: 17055429]

Kotake Y, Cao R, Viatour P, Sage J, Zhang Y, Xiong Y. pRB family proteins are required for H3K27 trimethylation and Polycomb repression complexes binding to and silencing $p16^{INK4a}$ tumor suppressor gene. Genes Dev. 2007; 21:49–54. [PubMed: 17210787]

Kotake Y, Zeng YX, Xiong Y. DDB1-CUL4 and MLL1 mediate oncogene-induced p16(INK4a) activation. Cancer Res. 2009; 69:1809–1814. [PubMed: 19208841]

Krimpenfort P, Ijpenberg A, Song JY, van der Valk M, Nawijn M, Zevenhoven J, et al. p15Ink4b is a critical tumour suppressor in the absence of p16Ink4a. Nature. 2007; 448:943–946. [PubMed: 17713536]

Krimpenfort P, Quon KC, Mooi WJ, Loonstra A, Berns A. Loss of $p16^{Ink4a}$ confers susceptibility to metastatic melanoma in mice. Nature. 2001; 413:83–86. [PubMed: 11544530]

Krishnamurthy J, Torrice C, Ramsey MR, Kovalev GI, Al-Regaiey K, Su L, et al. Ink4a/Arf expression is a biomarker of aging. J Clin Invest. 2004; 114:1299–1307. [PubMed: 15520862]

Malumbres M, Perez De Castro I, Hernandez MI, Jimenez M, Corral T, Pellicer A. Cellular response to oncogenic ras involves induction of the Cdk4 and Cdk6 inhibitor p15(INK4b). Mol Cell Biol. 2000; 20:2915–2925. [PubMed: 10733595]

McPherson R, Pertsemlidis A, Kavaslar N, Stewart A, Roberts R, Cox DR, et al. A common allele on chromosome 9 associated with coronary heart disease. Science. 2007; 316:1488–1491. [PubMed: 17478681]

Nagano T, Mitchell JA, Sanz LA, Pauler FM, Ferguson-Smith AC, Feil R, et al. The Air noncoding RNA epigenetically silences transcription by targeting G9a to chromatin. Science. 2008; 322:1717–1720. [PubMed: 18988810]

Pandey RR, Mondal T, Mohammad F, Enroth S, Redrup L, Komorowski J, et al. Kcnq1ot1 antisense noncoding RNA mediates lineage-specific transcriptional silencing through chromatin-level regulation. Mol Cell. 2008; 32:232–246. [PubMed: 18951091]

Pasmant E, Laurendeau I, Heron D, Vidaud M, Vidaud D, Bieche I. Characterization of a germ-line deletion, including the entire INK4/ARF locus, in a melanoma-neural system tumor family: identification of ANRIL, an antisense noncoding RNA whose expression coclusters with ARF. Cancer Res. 2007; 67:3963–3969. [PubMed: 17440112]

Rinn JL, Kertesz M, Wang JK, Squazzo SL, Xu X, Brugmann SA, et al. Functional demarcation of active and silent chromatin domains in human HOX loci by noncoding RNAs. Cell. 2007; 129:1311–1323. [PubMed: 17604720]

Saxena R, Voight BF, Lyssenko V, Burtt NP, de Bakker PI, Chen H, et al. Genome-wide association analysis identifies loci for type 2 diabetes and triglyceride levels. Science. 2007; 316:1331–1336. [PubMed: 17463246]

Scott LJ, Mohlke KL, Bonnycastle LL, Willer CJ, Li Y, Duren WL, et al. A genome-wide association study of type 2 diabetes in Finns detects multiple susceptibility variants. Science. 2007; 316:1341–1345. [PubMed: 17463248]

Serrano M, Lee H-W, Chin L, Cordon-Cardos C, Beach D, DePinho RA. Role of the INK4a locus in tumor suppression and cell mortality. Cell. 1996; 85:27–37. [PubMed: 8620534]

Sharpless NE, Bardeesy N, Lee KH, Carrasco D, Castrillon DH, Aguirre AJ, et al. Loss of $p16^{Ink4a}$ with retention of $p19^{Arf}$ predisposes mice to tumorigenesis. Nature. 2001; 413:86–91. [PubMed: 11544531]

Sherr CJ. Tumor surveillance via the ARF-p53 pathway. Genes Dev. 1998; 12:2984–2991. [PubMed: 9765200]

Terranova R, Yokobayashi S, Stadler MB, Otte AP, van Lohuizen M, Orkin SH, et al. Polycomb group proteins Ezh2 and Rnf2 direct genomic contraction and imprinted repression in early mouse embryos. Dev Cell. 2008; 15:668–679. [PubMed: 18848501]

Visel A, Zhu Y, May D, Afzal V, Gong E, Attanasio C, et al. Targeted deletion of the 9p21 non-coding coronary artery disease risk interval in mice. Nature. 2010; 464:409–412. [PubMed: 20173736]

Wang L, Brown JL, Cao R, Zhang Y, Kassis JA, Jones RS. Hierarchical recruitment of polycomb group silencing complexes. Mol Cell. 2004; 14:637–646. [PubMed: 15175158]

Wutz A, Rasmussen TP, Jaenisch R. Chromosomal silencing and localization are mediated by different domains of Xist RNA. Nat Genet. 2002; 30:167–174. [PubMed: 11780141]

Yap KL, Li S, Munoz-Cabello AM, Raguz S, Zeng L, Mujtaba S, et al. Molecular interplay of the noncoding RNA ANRIL and methylated histone H3 lysine 27 by polycomb CBX7 in transcriptional silencing of INK4a. Mol Cell. 2010; 38:662–674. [PubMed: 20541999]

Zhao J, Sun BK, Erwin JA, Song JJ, Lee JT. Polycomb proteins targeted by a short repeat RNA to the mouse X chromosome. Science. 2008; 322:750–756. [PubMed: 18974356]

Zindy F, Quelle DE, Roussel MF, Sherr CJ. Expression of the $p16^{INK4a}$ tumor suppressor versus other INK4 family members during mouse development and aging. Oncogene. 1997; 15:203–211. [PubMed: 9244355]

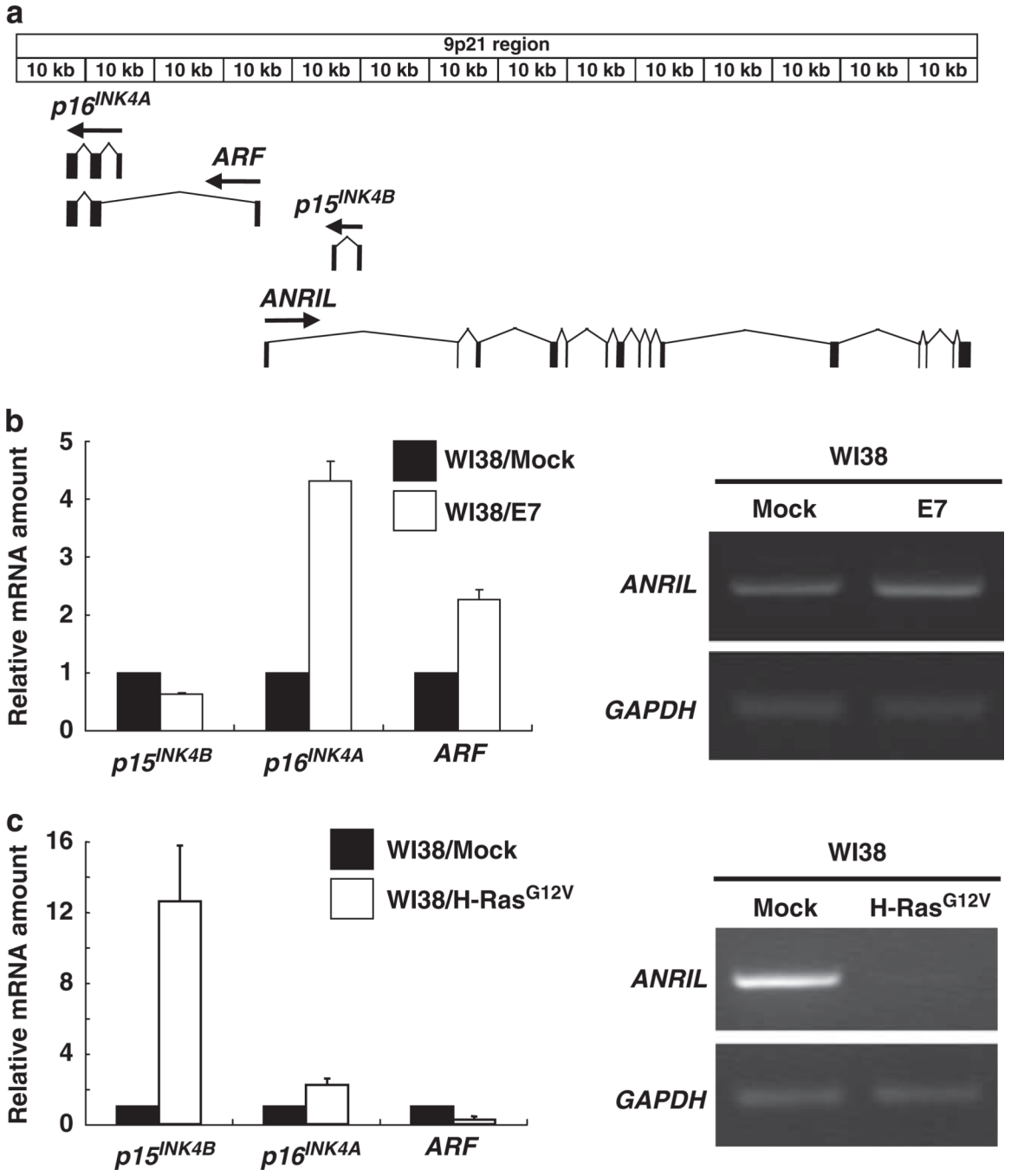

Figure 1. Oncogenic Ras inhibits the expression of *ANRIL* and stimulates $p15^{INK4B}$ expression

(**a**) Schematic representation of *INK4* locus. The arrows indicate the direction of transcription of each gene. The black boxes indicate the exons of *INK4* and *ANRIL* genes, respectively. (**b**) WI38 cells were infected with empty (Mock) or E7-expressing retroviruses and selected by 400 μg/ml G418 treatment as described in Kotake *et al.* (2007). (Left panel) The levels of $p15^{INK4B}$, $p16^{INK4A}$ and $p14^{ARF}$ mRNA were determined by quantitative reverse transcriptase PCR, and results are expressed relative to the corresponding values for WI38/Mock cells. The mean values and s.d.s were calculated from triplicates of a representative experiment. The specific PCR pairs for $p15^{INK4B}$, $p16^{INK4A}$, *ARF* and *GAPDH* are described in Kotake *et al.* (2007). (Right panel) The expression of *ANRIL* was

determined by reverse transcriptase PCR using primers designed on exon1 (forward primer) and exon2 (reverse primer) as described in the Supplementary Information. (**c**) WI38 cells were infected with empty (Mock) or oncogenic H-Ras^{G12V}-expressing retroviruses, selected by 2 μg/ml puromycin treatment for 3 days and harvested 8 days after initial infection. (Left panel) The levels of *p15*^{INK4B}, *p16*^{INK4A} and *p14*^{ARF} mRNA were determined by quantitative reverse transcriptase PCR, and results are expressed relative to the corresponding values for WI38/Mock cells. The mean values and s.d.s were calculated from triplicates of a representative experiment. (Right panel) The expression of *ANRIL* was detected by reverse transcriptase PCR using the same primers with (**b**).

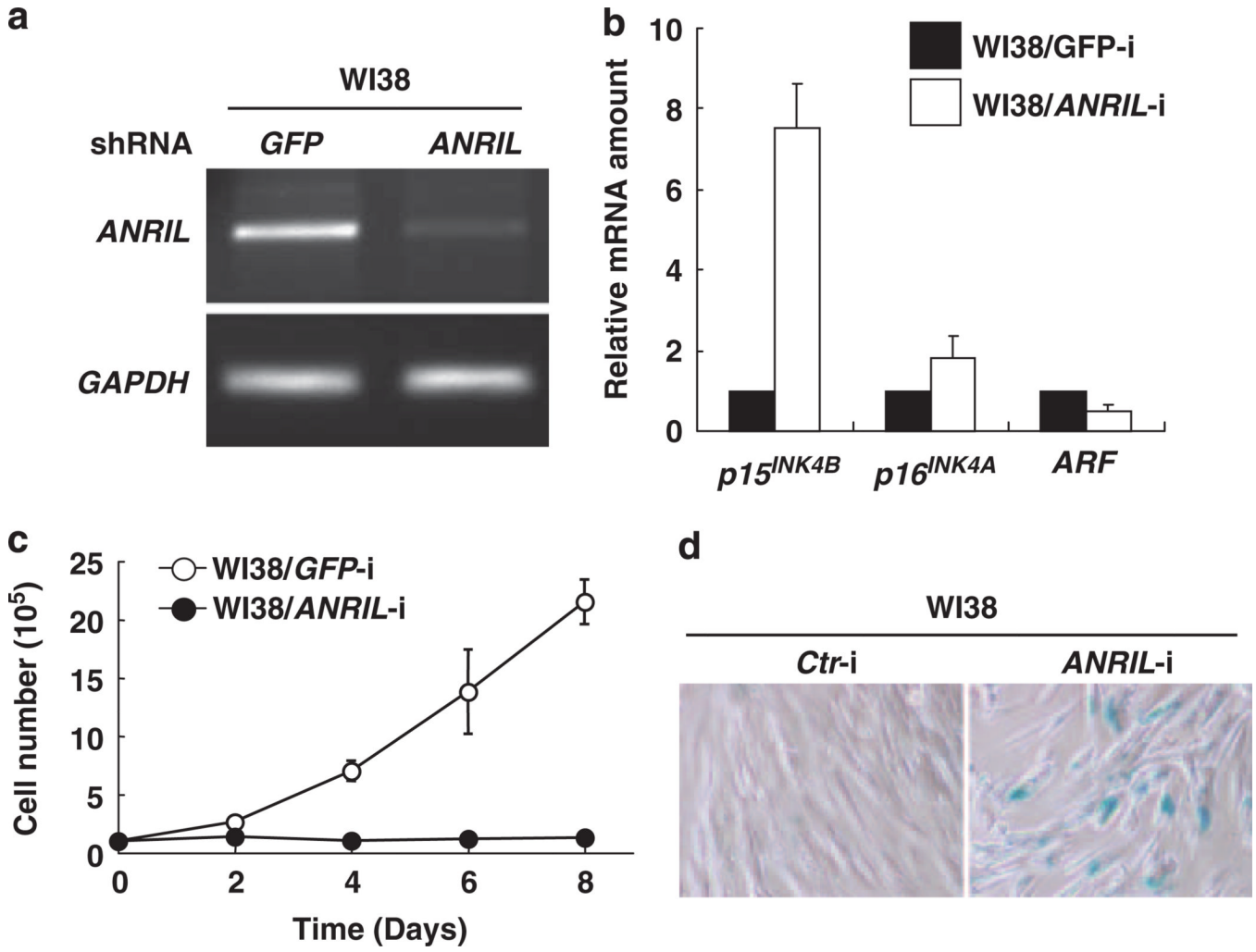

Figure 2. *ANRIL* negatively regulates $p15^{INK4B}$ gene expression

(**a**) WI38 cells were infected with a retrovirus vector encoding short hairpin RNA (shRNA) against either *GFP* or *ANRIL*, selected by 2 μg/ml puromycin treatment for 3 days and harvested 8 days after initial infection. The efficiency of *ANRIL* silencing was determined by reverse transcriptase PCR. (**b**) The effects of *ANRIL* silencing on $p15^{INK4B}$, $p16^{INK4A}$ and $p14^{ARF}$ were determined by quantitative reverse transcriptase PCR. The results are expressed relative to the corresponding values for WI38/GFP-i cells. The mean values and s.d.s were calculated from triplicates of a representative experiment. (**c**) The growth curves of WI38 cells infected with a retrovirus expressing shRNA against either GFP or *ANRIL*. Viable cells were counted by trypan blue staining at indicated days after initial seeding of 1×10^5 cells. (**d**) WI38 cells with small interfering RNA targeting either control or *ANRIL* were stained for senescence-associated β-galactosidase by using Senescence Detection Kit (BioVision, Mountain View, CA, USA).

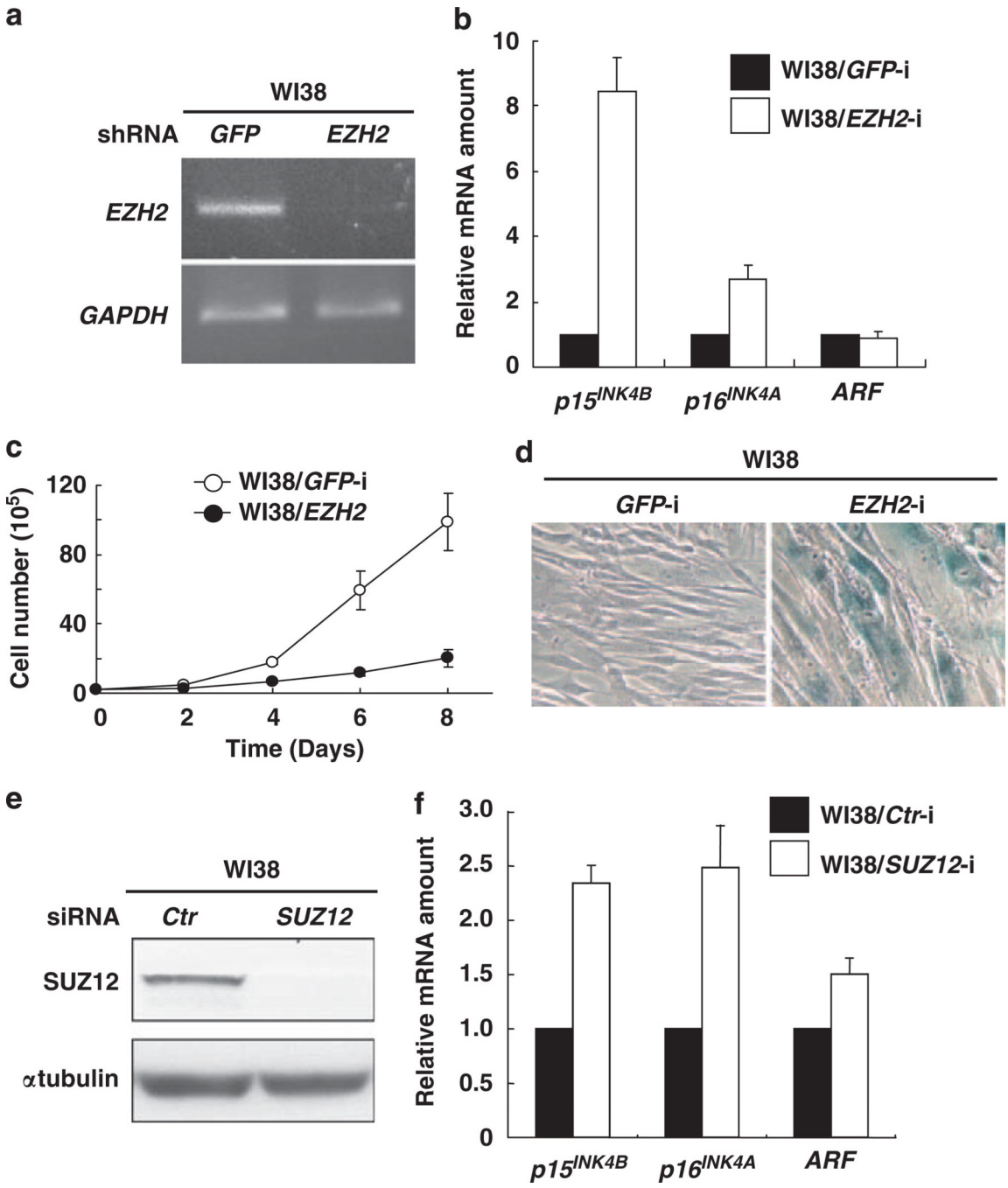

Figure 3. PRC2 binds to and negatively regulates *p15*^{INK4B} gene expression

(**a**) WI38 cells were infected with retrovirus expressing short hairpin RNA (shRNA) against either *GFP* or *EZH2*, selected by 2 μg/ml puromycin treatment and harvested 8 days after initial infection. The efficiency of *EZH2* silencing was determined by reverse transcriptase PCR. The specific PCR pair for *EZH2* is described in the Supplementary Information. (**b**) The effects of *EZH2* silencing on *p15*^{INK4B}, *p16*^{INK4A} and *p14*^{ARF} were determined by quantitative reverse transcriptase PCR, and results are expressed relative to the corresponding values for WI38/GFP-i cells. The mean values and s.d.s were calculated from triplicates of a representative experiment. (**c**) The growth curves of WI38 cells infected with a retrovirus expressing shRNA against either *GFP* or *EZH2*. Viable cells were counted by

trypan blue staining at indicated days after initial seeding of 2×10^5 cells. (**d**) WI38 cells infected with a retrovirus expressing shRNA against either *GFP* or *EZH2* were stained for senescence-associated β-galactosidase. (**e**) The efficiency of *SUZ12* silencing by small interfering RNA (siRNA) was determined by immunoblotting. Antibodies to SUZ12 (Millipore, Billerica, MA, USA) and αtubulin (Sigma, St Louis, MO, USA) were purchased commercially. (**f**) The effects of *SUZ12* silencing on $p15^{INK4B}$, $p16^{INK4A}$ and $p14^{ARF}$ were determined by quantitative reverse transcriptase PCR.

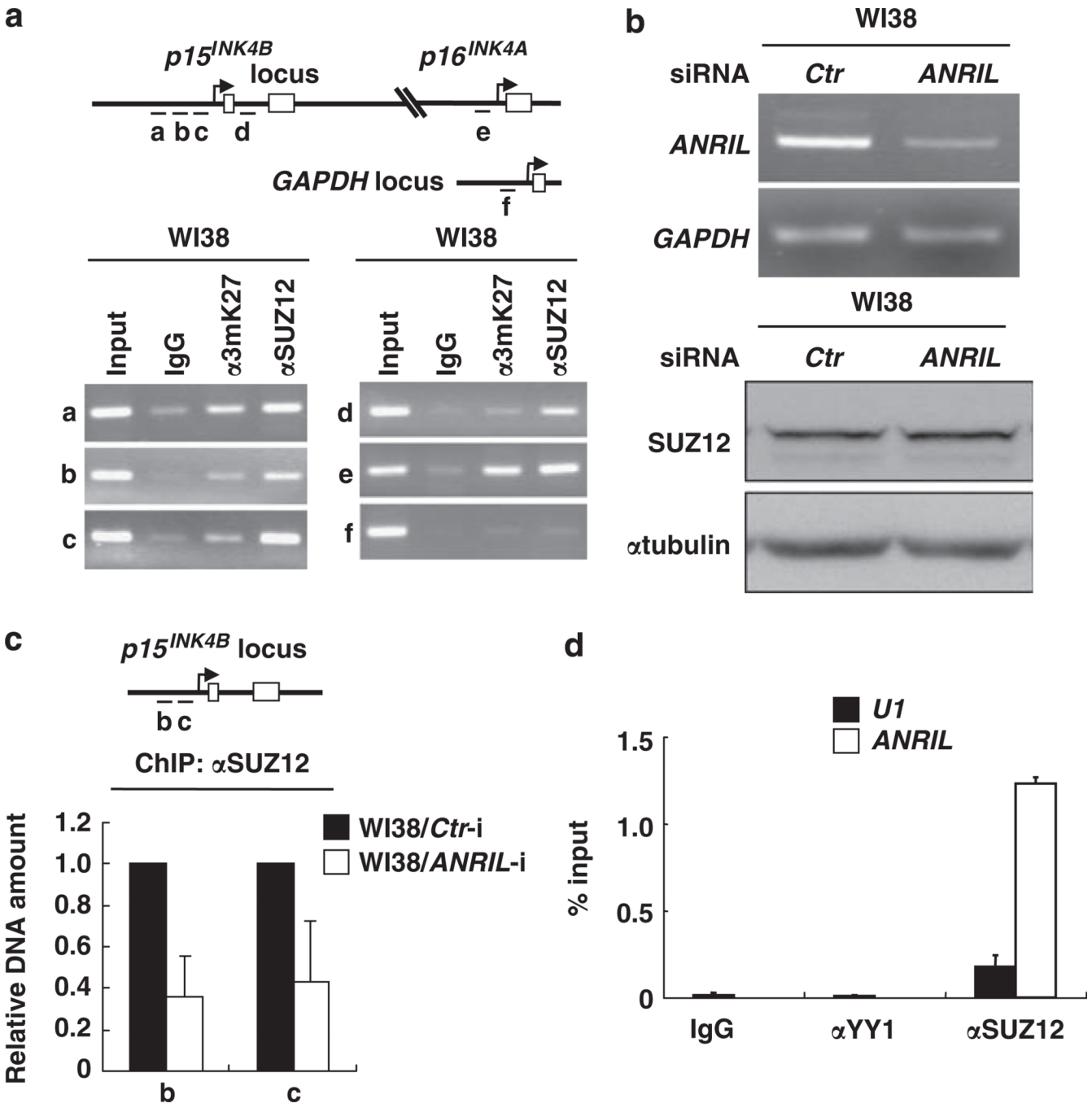

Figure 4. *ANRIL* binds to and is required for the recruitment of SUZ12 to $p15^{INK4B}$ locus

(**a**) A schematic representation of the $p15^{INK4B}$, $p16^{INK4A}$ and *GAPDH* gene loci and amplicons (a–f) used for chromatin immunoprecipitation assay. Antibodies against SUZ12, trimethyl-H3K27 and immunoglobulin G (IgG) control were used in the chromatin immunoprecipitation assay. PCR was carried out using primers for each amplicon. The sequence of primer pairs is described in the Supplementary Information. (**b**) The efficiency of *ANRIL* silencing by small interfering RNA (siRNA) was determined by reverse transcriptase PCR. The SUZ12 protein level was determined by immunoblotting. (**c**) A schematic representation of the $p15^{INK4B}$ locus and amplicons (b and c). Abundance of SUZ12 binding on the $p15^{INK4B}$ locus was determined by quantitative PCR following

chromatin immunoprecipitation assay with SUZ12 antibody in WI38 cells with siRNA targeting either control or *ANRIL*. PCR was carried out using primers for each amplicon. (**d**) Nuclear extracts of WI38 cells were immunoprecipitated by IgG, anti-SUZ12 or anti-YY1. Coprecipitated RNAs were detected by quantitative reverse transcriptase PCR using primers for *ANRIL* (derived from exons 1 and 2) or U1 small nuclear RNA as described in the Supplementary Information. The results are expressed relative to the corresponding values for input RNAs. The mean values and s.d.s were calculated from triplicates of a representative experiment.